LA-UR- 02-7006

Approved for public release; distribution is unlimited.

Title: HYDRATION AND MOBILITY OF HO-(AQ)

Author(s): Dilipkumar Asthagiri, 185000, T-12
Lawrence R. Pratt, 098754, T-12
Joel D. Kress, 103079, T-12
Maria A. Gomez, Vassar College

Submitted to: Proceedings of the International Academy of Science

Los Alamos
NATIONAL LABORATORY

Hydration and mobility of $HO^-(aq)$

D. Asthagiri, Lawrence R. Pratt, and J. D. Kress
Theoretical Division, Los Alamos National Laboratory, Los Alamos, NM 87545

Maria A. Gomez
Department of Chemistry, Vassar College, Poughkeepsie, NY, 12604
(Dated: October 31, 2002)

The hydroxide anion plays an essential role in many chemical and biochemical reactions. But questions of its hydration state and transport in water are currently controversial. Here we address this situation using the quasi-chemical theory of solutions. The simplest such approach suggests that $HO \cdot [H_2O]_3^-$ is the most probable species at infinite dilution in aqueous solution under standard conditions, followed by the $HO \cdot [H_2O]_2^-$ and $HO \cdot [H_2O]^-$ forms which are close together in stablity. $HO \cdot [H_2O]_4^-$ is less stable, in contrast to recent proposals that the latter structure is the most stable hydration species in solution. *Ab initio* molecular dynamics results presented here support the dominance of the tri-hydrated form, but that the population distribution is broad and sensitive to solution conditions. On the basis of these results, the mobility of hydroxide can be simply that of a proton hole. This contrasts with recent proposals invoking the interconversion of a stable 'trap' structure $HO \cdot [H_2O]_4^-$ to $HO \cdot [H_2O]_3^-$ as the rate determining step in the transport process.

I. INTRODUCTION

A pre-eminent challenge in liquid state physics is the understanding of aqueous systems and the reactions there. Water undergoes limited autoprotolysis, which is enhanced in the presence of highly charged metals such as Be^{2+}. Beryllium induced autoprotolysis has consequences for the speciation of this metal(in water [1]), with implications for environmental clean-up strategies, and in understanding how inhaled beryllium dust leads to chronic beryllium disease [2]. Foundational to these issues is to first understand $HO^-(aq)$ which serves as a cross-linker in multinuclear beryllium clusters.

The anomolous diffusion of the $H^+(aq)$ and $HO^-(aq)$ has received extensive scrutiny over the years (for example, [3, 4]). These studies all contained nuggets of insight that remain to this day. Recently, *ab initio* molecular dynamics (AIMD) has provided new information on the solution condition and transport of these species. Over a similar time scale, the statistical mechanical theory of liquids (especially water) has also become usefully more sophisticated. (for example, [5, 6]). These two approaches can be complementary, but in typical practice they remain unfortunately disconnected (but see [7–10]).

In an initial AIMD study [11, 12], $HO^-(aq)$ was observed to be tetra-hydrated during the course of the ~6 ps long simulation. This complex had a lifetime of about 2-3 ps there. The structure of this complex ($HO \cdot [H_2O]_4^-$) involved four water molecules in a roughly square, planar arrangement with the HO^- group coordinating the water molecules in a pin-wheel type configuration. That study hinted that the transport occurred when $HO \cdot [H_2O]_4^-$ converted to a tri-hydrated ($HO \cdot [H_2O]_3^-$) species in which the ligating water molecules are arranged roughly as three corners of a tetrahedron centered on the anion oxygen, similar to the hydrogen bonding arrangements in water.

A more recent study [13] reinforces the notion of a stable $HO \cdot [H_2O]_4^-$ species. The proposed mechanism for $HO^-(aq)$ transport is: first the stable (and hence "inactive") $HO \cdot [H_2O]_4^-$ converts to the "active" $HO \cdot [H_2O]_3^-$ species; then the H-bond between the anion and one of the ligating water molecules shortens, thus identifying a transient $HO \cdot [H_2O]^-$ species; a shared proton is transferred along that shortened bond, and a $HO \cdot [H_2O]_3^-$ species is reconstituted with the hydroxide identity now switched; this "active" $HO \cdot [H_2O]_3^-$ species reverts back to an "inactive" $HO \cdot [H_2O]_4^-$ moiety completing one transport event. Statistical characterization has sketchy but presumably, as in [12], the lifetime of the $HO \cdot [H_2O]_4^-$ species could be about 2-3 ps, so that in about 60 ps of simulation [13], 20-30 transport events might be anticipated.

Discussions of a transport mechanism for $HO^-(aq)$ typically focus on Agmon's[14, 17] extraction of an activation energy for hydroxide transport from the temperature dependence of the experimental mobilities. Near room temperature that empirical parameter is about 3 kcal/mol but increases by roughly a factor of two for slightly lower temperatures. As a mechanical barrier this value, about 5-6 kT, may be low enough to require some subtlety of interpretation[15]; the observed temperature sensitivity supports that possibility. But Tuckerman *et al.* [13] estimate the barrier height for their proposed mechanism as follows: (A) Novoa et al. [16] in a gas-phase calculation find a barrier height of 1.16 kcal/mole for the conversion of $HO \cdot [H_2O]_4^-$ to $HO \cdot [H_2O]_3^-$ — the first shell hydrating water moves to the second shell; [Note that, in order to be interpreted as a free energy for that comparison in liquid water, this value must be density dependent to reflect the fugacity of water molecule ligands.] (B) Agmon [14] estimates a value of 0.5 kcal/mole for shortening of one (1) H-bond pair which they multiply by three (3) for the three H-bonds to HO^- in $HO \cdot [H_2O]_3^-$; (C) then they combine this with 0.34 kcal/mole, a path integral estimate (involving the entire simulation sys-

tem) for the activation energy for proton transfer between the two tri-hydrated species transiently involving $HO \cdot [H_2O]^-$. The combined estimate of 3 kcal/mole was noted to be consistent with the value quoted by Agmon for his quite different mechanism for HO^- transport. In his model, the water molecule hydrating $HO \cdot [H_2O]_3^-$ — the second shell water — first dissociates, costing about 2.6 kcal/mole. Then one (1) of the O-O bond shortens, which he estimates to cost 0.5 kcal/mole, and a proton transfer occurs. Agmon thus gets a combined estimate of 3.1 kcal/mole.

This target activation energy estimates were based on bulk property measurements [17] and these empirical coefficients of exponents of $1/T$ include a solvent influence. Additionally, the earlier gas-phase studies have shown that (a) $HO \cdot [H_2O]_3^-$ is *stabler* than $HO \cdot [H_2O]_4^-$, and (b) the barrier for $HO \cdot [H_2O]_3^-$ to $HO \cdot [H_2O]_4^-$ is 2.5 kcal/mole, nearly 1.3 kcal/mole *greater* than the barrier for the reverse process. This is only 0.5 kcal/mole off the 3 kcal/mole estimate in [13].

The apparent inconsistencies of these various results were noted recently [18]. Those AIMD studies treated NaOD and KOD solutions with concentrations ranging between 1.5 M to 15 M [18, 19]. Interestingly, they showed that $HO \cdot [H_2O]_3^-$ was also well-represented in the population distribution though this distribution was influenced by the counterion. Yet $HO \cdot [H_2O]_4^-$ was still found to be the most probable hydration structure and the transfer pathway suggested by [13] was strengthened.

The observed influence of the cations in those more recent calculations[18] means that solution condition of a solitary HO^-(aq) is not settled and the original speculations therefore not resolved. We use two distinct approaches to address these issues. Both our statistical mechanical quasi-chemical theory of solutions and preliminary AIMD simulations suggest that $HO \cdot [H_2O]_3^-$ is the stable species. The simulations suggest that transport of the hydroxide is similar to the transport of a proton hole. We suggest how the apparent high "effective" solvation number of HO^- can be resolved without invoking $HO \cdot [H_2O]_4^-$.

II. QUASI-CHEMICAL THEORY

In the quasi-chemical theory [6], the region around the solute of interest is partitioned into an inner shell and outer shell domains. Typically the inner shell, where chemical effects could be important, is treated quantum mechanically. The outer shell contributions can be assessed using classical force-fields or dielectric continuum models. (The theory permits a variational check of this partition.) In the present study outer shell contributions have been evaluated with a dielectric continuum model and the trends confirmed by molecular dynamics calculations using classical interatomic potentials.

The inner shell reactions are:

$$HO^- + nH_2O \rightleftharpoons HO[H_2O]_n^-$$

The free energy change for these reactions were calculated using the Gaussian programs [20]. The $HO \cdot [H_2O]_n^-$ (n = 0...4) clusters were geometry optimized in the gas phase using the B3LYP hybrid density functional[?] and the 6-31+G(d,p) basis set. Frequency calculations confirmed a true minimum, and the zero point energies were computed at the same level of theory. Single point energies were calculated using both the 6-311+G(2d,p) and the aug-cc-pVTZ basis sets. For estimating the outer shell contribution, the ChelpG method [21]) was used to obtain partial atomic charges. Then with the radii set developed by Stefanovich et al.[22], surface tessera generated [23], and the solvation free energies of the clusters calculated using a dielectric continuum model [24]. With this information and the binding free energies for the chemical reactions, the quasi-chemical approximation to the excess chemical potential of HO^-(aq) in water can be written as:

$$\beta\mu^{ex}_{OH^-(aq)} \approx -\ln\left(1 + \sum_{n\geq 1} \tilde{K}_n \rho_{H_2O}{}^n\right) \qquad (1)$$

where $\tilde{K}_n = K_n{}^{(0)} \exp\left[-\beta\left(\mu^{ex}_{HO(H_2O)_n^-} - n\mu^{ex}_{H_2O}\right)\right]$. $K_n{}^{(0)}$ is the equilibrium constant for the reaction in an ideal gas state. (Although the theory requires binding constants in solution phase, a primitive first approximation is to use these gas phase quantities.) The density term appearing in eq. 1 reflects the actual density of liquid water and its effect is accounted for by including a replacement contribution of $-nRT\ln(1354)$. It is this replacement contribution reflecting the availability of water molecule ligands that was noted earlier as missing from the conventional electronic energy differences discussed above. A detailed statement on standard states and this replacement contribution can be found in Grabowski et al. [10].

Figure 1 gives the solvation free energy of the hydroxide anion for various hydration states. The excess free energies were calculated assuming only one particular n in eq. 1 to better highlight μ^{ex} vs. n dependency. It is clear, however, that based on the exponential weighting in K_n that including $n = 1, 2, 3$ would be indistinguishable from using just $n = 3$. Clearly including $n = 4$ will make no difference. In decreasing order of stability, the order $HO \cdot [H_2O]_3^- > HO \cdot [H_2O]_2^- \sim HO \cdot [H_2O]^- > HO \cdot [H_2O]_4^-$ is found. This result is contrary to the apparent stability of $HO \cdot [H_2O]_4^-$ inferred in earlier AIMD simulations. The solvation free energy estimate between (-)103-105 kcal/mole is in good agreement with recently suggested values [25]. The a more general discussion such single ion hydration free energies will be presented elsewhere (Asthagiri, Ashbaugh, and Pratt; in preparation).

To check limitations of the dielectric model of outer shell contributions, the charging free energies of $HO \cdot [H_2O]_3^-$ and $HO \cdot [H_2O]_4^-$ were obtained using classical molecular dynamics approach. We found that $\mu^{ex}_{HO\cdot[H_2O]_3^-} - \mu^{ex}_{HO\cdot[H_2O]_4^-} = -6.9$ kcal/mole in reason-

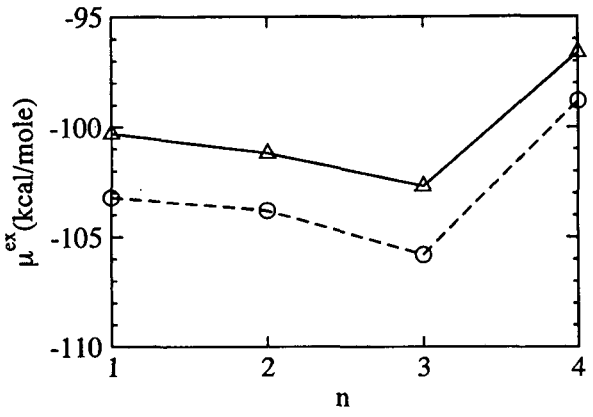

FIG. 1: Quasi-chemical estimate of the solvation free energy of HO^-(aq). n is the number of inner shell water molecules surrounding the anion. △, calculations with B3LYP/aug-cc-pVTZ; ○, calculations with B3LYP/6-311+G(2d,p). An observation volume of radius 1.7 Å centered on the anionic oxygen defined the inner shell. Using 2.0 Å instead did not lead to significant changes.

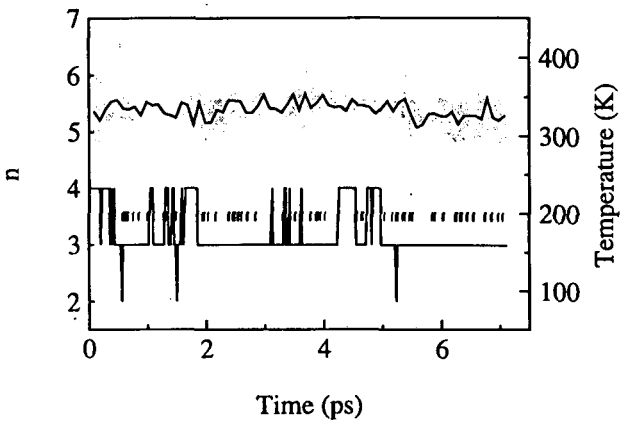

FIG. 2: Coordination number and temperature versus time. The block averaged temperature, with block size of 50 fs, is shown with the solid line. The mean temperature is 335±21 K. The coordination number counts the number of hydrogen (H) atoms surrounding the hydroxide oxygen (O*), excluding the HO^- hydrogen. The inner shell is defined by $R(O^*H) \leq 2.0$. The short vertical bars at the $n = 3.5$ level flag hydrogen exchange events in which the identity of the hydroxide oxygen is changed. Note that many hydrogen exchange events occur without intercession of an n=4 configuration. Simulation details with predominant coordination number in parethesis: ~10 ps classical MD ($n = 5$), followed by ~1.5 ps of velocity scaling AIMD ($n = 4$), and followed by the above NVE ensemble simulations. The total energy stayed ±0.22 (2σ) eV (or ±0.26 k_bT per heavy atom) of the mean.

able agreement with the -6 kcal/mole found using a dielectric model. Importantly, the trend is unaltered. (Note that we did not attempt to obtain new parameters for the quasi-component water interaction, but have used the same oxygen parameters as in the water model.) Positive outer shell packing contributions are not addressed here, but these are expected to be slightly larger for $HO \cdot [H_2O]_4^-$ than for $HO \cdot [H_2O]_3^-$ and hence should enhance the calculated difference.

The energetics for the gas-phase hydration reactions, and the cluster structures, are in reasonable agreement with results in [26], with differences attributable to differences in the basis sets for optimization and energy evaluations.

III. AB INITIO MOLECULAR DYNAMICS

The AIMD simulations were carried out with the VASP simulation program using generalized gradient approximation to the electron density functional theory. Ultrasoft pseudopotentials for oxygen were used to describe the core-valence interaction, and the valence orbitals were expanded in plane waves with a kinetic energy cutoff of 29.1 Ry. The system comprises a hydroxide anion in a box of 32 water molecules. The box size was set to 9.8788 Å consistent with the experimental partial specific volume of the HO^-(aq) [27]. This system was initially thermalized by about 10 ps of classical molecular dynamics simulation with a temperature of 300 K using periodic velocity scaling. All our AIMD simulations were performed with 1 fs timestep, which is fairly conservative. This choice is validated by the excellent energy conservation during the NVE simulations (figs. 2 and 3).

In the earlier CP-AIMD approach, the wave function optimization was sought using Newtonian dynamics in which the electrons are assigned a fictitious mass. A recent study [28] of CP-AIMD suggested "... the necessity for checking the dependence of results of CP simulations on the value of the fictitious mass parameter" because they found a constant bias, in proportion to the fictitious electron mass, between the force based on the Born-Oppenheimer surface (the Hellmann-Feynman force on the nuclei) and the CP-Lagrangian derived force. Bear in mind, however, that in our AIMD simulations the wave functions are converged for each nuclear position by conjugate gradient methods; so if the wave function converges at all, it will converge to the BO-surface. For all but the first step, this convergence is achieved in 4 SCF cycles, and in 5-6 cycles for proton-sharing situations between two HO^- groups, but never more.

Fig. 2 shows that starting from about 1.5 ps of velocity scaling AIMD simulation and removing the thermostat led to a rise in temperature. Interestingly within the first 300 fs the $HO \cdot [H_2O]_4^-$ structure converts to the $HO \cdot [H_2O]_3^-$ structure. This structure is predominant, although $HO \cdot [H_2O]_4^-$ is also statistically represented. In fig. 2 the bars flag the exchange of hydroxide identity between the preceeding 20 fs block and the succeeding

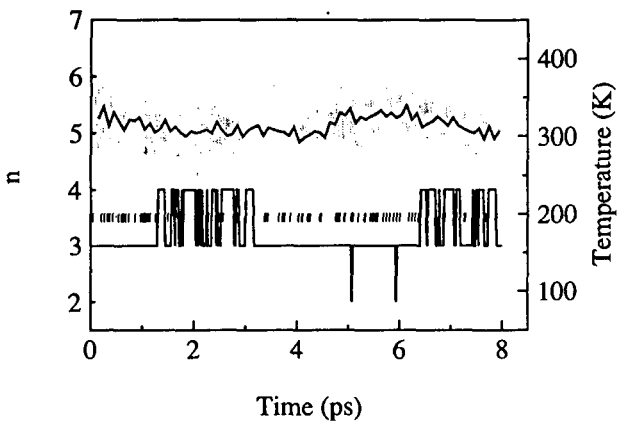

FIG. 3: Coordination number and temperature versus time. The block averaged temperature, with block size of 50 fs, is shown with the solid line. The mean temperature is 314±21 K. The coordination number counts the number of hydrogen (H) atoms surrounding the hydroxide oxygen (O^*), excluding the HO^- hydrogen. The inner shell is defined by $R(O^*H) \leq 2.0$. The bars at $n = 3.5$ flag hydoxyl exchange events. Simulation details with predominant coordination number in parenthesis: ~10 ps classical MD ($n = 5$), followed by ~1.5 ps of velocity scaling AIMD ($n = 4$), followed by ~1.5 ps of NVE ensemble simulations ($n = 3$) as in fig. 2. Then a configuration was extracted and random velocities assigned at a of 300 K. This was followed by the NVE run shown. The total energy stayed within ± 0.15 (2σ) eV.

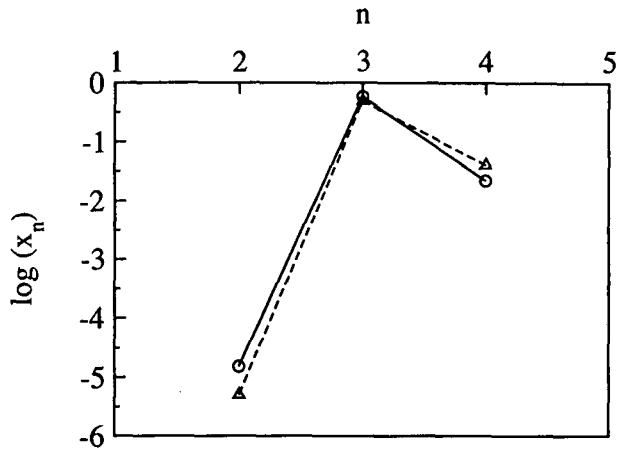

FIG. 4: $\ln x_n$ versus the coordination number. x_n is the fraction of the population with n inner shell water molecules. o, statistics from fig. 2; △, statistics from fig. 3.

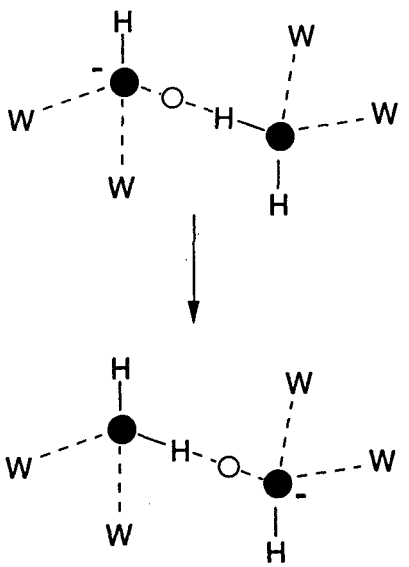

FIG. 5: A schematic of the hole movement. o denotes the hole and • the oxygen centers. Hydrating water molecules are simply denoted by w. The AIMD trajectories are available upon request.

20 fs block (the stored configurations were re-sampled every 20 fs). It is immediately obvious that the proton transfer involves only the $HO \cdot [H_2O]_3^-$ structure, which was noted as the active structure in [13, 19]. No interconversion between $HO \cdot [H_2O]_4^-$ and $HO \cdot [H_2O]_3^-$ appears to mediate transport. Further in the ca. 5.5 ps of simulations the mean lifetime of $HO \cdot [H_2O]_4^-$ is clearly shorter than the 2-3 ps.

The results in fig. 3 reinforces the predominance of $HO \cdot [H_2O]_3^-$, although, as before, $HO \cdot [H_2O]_4^-$ is statistically represented. The proton transfers are again between $HO \cdot [H_2O]_3^-$ species, with no mediation of $HO \cdot [H_2O]_4^-$.

It is instructive to consider the x_n distribution (fig. 4). From fig. 4, $-RT \ln(x_3/x_4) \approx -1$ kcal/mole. This is significantly less than the ≈-6 kcal/mole suggested by the primitive quasi-chemical approach, but the ordering is correct. Also clearly $n = 2$ is predicted to be significantly less stable in contrast to the quasi-chemical prediction. A source of concern in the analysis in fig. 4 is the lack of sufficient statistics, a problem that vexes AIMD simulations. Futher, for $n = 4$ say, a range of structures will be represented in the AIMD simulation, but only the stablest structure is used in the primitive quasi-chemical approximation. It is possible to include these other structures but obtaining these structures in the gas-phase is daunting. The x_2 statistic is artifactual as will be discussed below. Note that quasi-chemical theory can be formulated in terms of these x_n distributions, but practical applications decidedly suffer from limited statistics in AIMD simulations [9].

IV. CONCLUDING DISCUSSIONS

Two distinct lines of theoretical investigation converge to a common view: the $HO \cdot [H_2O]_3^-$ species is the stabler form. The transport mechanism simply involves the movement of the hole between two tri-hydrated centers as idealized in fig. 5. There certainly are second-shell

rearrangements, but not the large scale breaking and reforming of hydrogen bonds suggested by Agmon[14]. It appears that simple distortions of H-bonds are what are occuring on the timescales of the hole movement. Once the hole settles into its new place there will certainly be rearrangements.

It thus appears that if one discards the notion of a freely rotating water from Bernal and Fowler's proposal [3], then their idea of hole-hopping is essentially correct. Such hole-hopping was also considered by Stillinger[5] in his statistical mechanical development of proton transfer processes. Critically, no rate limiting changes in the inner shell hydration structure of the HO^-(aq) mediating transport is noted.

An interesting result from the simulations is the average O-O distance between the anionic oxygen and the nearest neighboring oxygen atom: $2.47\pm0.12(2\sigma)$ Å in fig. 2 and $2.46\pm0.1(2\sigma)$ Å in fig. 3. This distance is surprisingly close to O-O separation in the gas-phase structure of $HO\cdot[H_2O]^-$. This then suggests that $HO\cdot[H_2O]^-$ is a prominent sub-grouping in the $HO\cdot[H_2O]_n{}^-$ $(n = 3, 4)$ species. This is the reason why x_1 cannot be unambiguously obtained and underlies the artifact noted in discussing fig. 4. Evidently, this grouping mediates the hole transport as sketched in fig. 5.

The presence of the $HO\cdot[H_2O]^-$ sub-grouping could resolve the high "effective" (not microscopic) hydration numbers extracted from dielectric dispersion measurements [29]. A 'super'-grouping of $HO\cdot[H_2O]^-$, one involving four (4) or more water molecules rather than HO^- alone, could well be relevent to time scale of the measurement. This possibility was also suggested by Agmon[14]. Then $HO\cdot[H_2O]_4{}^-$ [13, 18, 19] is not a consequence necessary to resolution of experimentally obtained "effective" hydration numbers.

Experimentalists have explained the spectroscopic features in concentrated ($> 2.5M$) alkaline solutions by invoking the $HO\cdot[H_2O]^-$ grouping [30–33]. It remains to be seen if this holds true at more modest concentrations ($< 1.5M$). The simulations here also show that the hydrogen of HO^- is not hydrogen bonded for most of the simulation. Spectroscopists infer the existence of this "free" OH stretch based on the spike in the Raman spectrum at $\sim$3600 cm^{-1}. It is attractive to speculate that the phonon-proton coupling [32] that is thought to lead to the characteristic IR-spectra also holds the key to understanding the hole transport rate (a similar situation holds for excess protons), but fundamentally it appears that there is no need to postulate new mechanisms for HO^- transport.

V. ACKNOWLEDGEMENTS

The work at Los Alamos was supported by the US Department of Energy, contract W-7405-ENG-36, under the LDRD program at Los Alamos. The work at Vassar was supported by a Camille and Henry Dreyfus Faculty Start-up Grant Program for Undergraduate Institutions. LA-UR-02-xxx

[1] Cecconi, F.; Ghilardi, C. A.; Ienco, A.; Mariani, P.; Mealli, C.; Midollini, S.; Orlandini, A.; and Vacca, A. *Inorg. Chem.* **2002**, *41*, 4006.
[2] Scott, B. L.; Wang, Z.; Marrone, B. L.; and Sauer, N. L. *J. Am. Chem. Soc.* **submitted**.
[3] Bernal, J. D. and Fowler, R. H. *J. Chem. Phys.* **1933**, *1*, 515.
[4] Eigen, M. *Angew. Chem. Intl. Ed.* **1964**, *3*, 1.
[5] Stillinger, F. H. In Eyring, H. and Henderson, D., editors, *Theoretical chemistry: Advances and Perspectives*, volume 3. Academic, New York, **1978**.
[6] Paulaitis, M. E. and Pratt, L. R. *Adv. Prot. Chem.* **2002**, *62*, in press.
[7] Geissler, P. L.; Dellago, C.; Chandler, D.; Hutter, J.; and Parrinello, M. *Science* **2001**, *291*, 2121.
[8] Rempe, S. B.; Pratt, L. R.; Hummer, G.; Kress, J. D.; Martin, R. L.; and Redondo, T. *J. Am. Chem. Soc.* **2000**, *122*, 966.
[9] Rempe, S. B. and Pratt, L. R. *Flu. Phase Eql.* **2001**, *183-184*, 121.
[10] Grabowski, P.; Riccardi, D.; Gomez, M. A.; Asthagiri, D.; and Pratt, L. R. *J. Phys. Chem. A* **2002**, *106*, 9145.
[11] Tuckerman, M.; Laasonen, K.; Sprik, M.; and Parrinello, M. *J. Phys. Chem.* **1995**, *99*, 5749.
[12] Tuckerman, M.; Laasonen, K.; Sprik, M.; and Parrinello, M. *J. Chem. Phys.* **1995**, *103*, 150.
[13] Tuckerman, M. E.; Marx, D.; and Parrinello, M. *Nature* **2002**, *417*, 925.
[14] Agmon, N. *Chem. Phys. Lett.* **2000**, *319*, 247.
[15] Drozdov, A. and Tucker, S. *J. Chem. Phys.* **2000**, *112*, 5251.
[16] Novoa, J. J.; Mota, F.; del Valle, C. P.; and Planas, M. *J. Phys. Chem. A* **1997**, *101*, 7842.
[17] Agmon, N. *J. Chim. Phys.* **1996**, *93*, 1714.
[18] Chen, B.; Ivanov, I.; Park, J. M.; Parrinello, M.; and Klein, M. L. *J. Phys. Chem. A* **2002**, *XXX*, 1.
[19] Chen, B.; Park, J. M.; Ivanov, I.; Tabacchi, G.; Klein, M. T.; and Parrinello, M. *J. Am. Chem. Soc.* **2002**, *124*, 8534.
[20] Frisch, M. J. *et al.* Gaussian 98 (Revision A.2), **1998**. Gaussian, Inc., Pittsburgh PA.
[21] Breneman, C. M. and Wiberg, K. B. *J. Comp. Chem.* **1990**, *11*, 361.
[22] Stefanovich, E. V. and Truong, T. N. *Chem. Phys. Lett.* **1995**, *244*, 65.
[23] Sanner, M. F.; Spehner, J.-C.; and Olson, A. J. *Biopolymers* **1996**, *38*, 305.
[24] Yoon, B. J. and Lenhoff, A. M. *J. Comp. Chem.* **1990**, *11*, 1080.
[25] Tissandier, M. D.; Cowen, K. A.; Feng, W. Y.; Gund-

lach, E.; Cohen, M. H.; Earhart, A. D.; Coe, J. V.; and TuttleJr, T. R. *J. Phys. Chem. A* **1998**, *102*, 7787.

[26] Chaudhuri, C.; Wang, Y.-S.; Jiang, J. C.; Lee, Y. T.; Chang, H. C.; and Niedner-Schatteburg, G. *Mol. Phys.* **2001**, *99*, 1161.

[27] Marcus, Y. *Ion solvation*. Wiley, London, **1985**.

[28] Tangney, P. and Scandolo, S. *J. Chem. Phys.* **2002**, *116*, 14.

[29] Buchner, R.; Hefter, G.; May, P. M.; and Sipos, P. *J. Phys. Chem. B* **1999**, *103*, 11186.

[30] Zatsepina, G. N. *Zhur. Struk. Khim. (English ed.)* **1971**, *12*, 894.

[31] Schiöberg, D. and Zundel, G. *J. Chem. Soc. Faraday Trans. II.* **1973**, *69*, 771.

[32] Librovich, N. B.; Sakun, V. P.; and Sokolov, N. D. *Chem. Phys.* **1979**, *39*, 351.

[33] Librovich, N. B. and Maiorov, V. D. *Russ. J. Phys. Chem.* **1982**, *56*, 380.